

[CASE REPORT]

Small Cystic Pancreatic Neuroendocrine Neoplasm with Huge Liver and Bone Metastases

Muneji Yasuda, Shotai Takeda, Minami Lee, Susumu Hoshi, Tomoko Hoshi, Yuichi Tanaka, Shinji Miyajima, Haruo Takaya and Kozo Kajimura

Abstract:

Pancreatic neuroendocrine neoplasms occasionally have a cystic component. We herein report a case of multiple hepatic tumors, including a huge one and a 24-mm sized pancreatic cystic lesion. The hepatic tumor showed an enhancement pattern consistent with hepatic adenoma. The pancreatic cystic lesion revealed a thickened outside border and a solid inside component, which was enhanced following a contrast study, suggesting cystic pancreatic neuroendocrine neoplasm. Surgical resection was performed. After the surgery, somatostatin receptor scintigraphy detected an occult lumbar spine metastasis. Huge multiple liver and bone metastases of the neuroendocrine neoplasm G2 component were seen, with a G1 small primary lesion.

Key words: pancreatic neuroendocrine neoplasm, cystic change, liver metastasis, endoscopic ultrasonography

(Intern Med 59: 3027-3032, 2020)

(DOI: 10.2169/internalmedicine.5038-20)

Introduction

Pancreatic neuroendocrine neoplasms (PNETs) have been regarded as a relatively rare disease. However, in recent years, there has been an increase in the number of reported incidences owing to the progress of diagnostic imaging. Some cases exhibit unusual imaging findings and unusual progression.

We herein report a case of a small, cystic PNET G1 with bulky G2 liver metastasis that had some uncommon features.

Case Report

We encountered a 37-year-old woman who complained of a persistent low-grade fever. She had been taking oral contraceptives for irregular periods for five years.

On an examination, she showed no abnormal findings except for a slight fever (37.1°C). Laboratory findings, including aspartate aminotransferase, alanine aminotransferase, amylase, carcinoembryonic antigen, carbohydrate antigen 19-9, α -fetoprotein, protein induced by vitamin K absence or antagonist-II, and progastrin-releasing peptide, were within normal ranges. Neuron-specific enolase was 24.5 ng/

mL (normal: ≥ 16.3 ng/mL).

A 10-cm mixed echoic hepatic nodule in the right lobe and a 2-cm cystic lesion with a septal wall in the pancreatic tail end were found on abdominal ultrasound. On multidetector computed tomography (MDCT), we observed a hepatic tumor showing heterogeneous hyperenhancement during the arterial phase and washout of the contrast enhancement during the delayed phase. The pancreatic cystic lesion seemed to have a capsule-like rim structure (Fig. 1). On T2-weighted imaging (T2WI) of magnetic resonance imaging (MRI), the hepatic tumor showed a high signal intensity and mild diffusion restriction on diffusion-weighted imaging and apparent diffusion coefficient imaging. The pancreatic lesion displayed a high signal and slit-shaped low signal on T2WI (Fig. 2). On gadolinium ethoxybenzyl diethylenetriamine-pentaacetic acid (Gd-EOB-DTPA) enhancement MRI (EOB-MRI), the hepatic tumor demonstrated early enhancement with a poor-contrast central scar-like structure and washout during the portal venous and hepatobiliary phases (20 min) (Fig. 3). Following the initial evaluation, we performed endoscopic ultrasonography (EUS) using an oblique viewing echoendoscope (UCT-260, Olympus, Tokyo, Japan). A 24-mm sized cystic lesion with lateral shadowing and isoechoic and anechoic components was observed. Communication be-

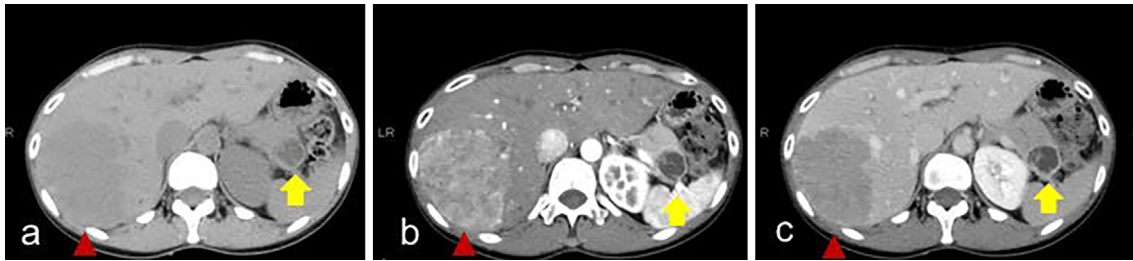


Figure 1. CT scan: a: The non-contrast phase showing a 10-cm low-density area in the posterior segment (triangle) and a 2-cm cystic lesion with capsule-like rim (arrow), b: the hepatic tumor showing heterogeneous hyper enhancement in the arterial phase, c: washout of the contrast enhancement during the delayed phase. The pancreatic lesion showing rim and intra-cystic component enhancement.

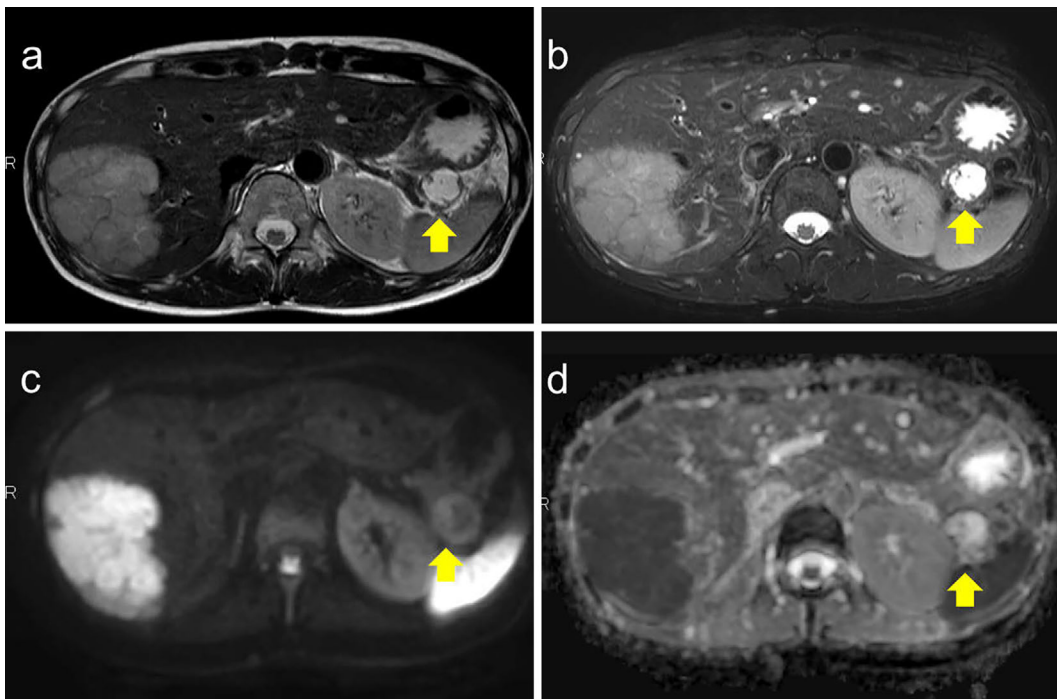


Figure 2. a: The pancreatic lesion (arrow) showing an intra-cystic slit-shaped component on T1WI, b: high signal on T2WI, c, d: no abnormal signal on diffusion-weighted or apparent diffusion coefficient imaging.

tween the cyst and the main pancreatic duct was not seen. Contrast-enhanced EUS using Sonazoid[®] (Daiichi-Sankyo, Tokyo, Japan) showed distinct enhancement in the outer border of the cystic wall and a solid inside component (Fig. 4). This lesion was suggestive of cystic degeneration of the solid neoplasm rather than the septal wall of cystic one.

At this point, we proposed several possible diagnoses for this hepatic tumor, including hepatic adenoma due to the blood supply pattern. Focal nodule hyperplasia (FNH) was also included in the differential diagnosis. As for the pancreatic lesion, PNEN with cystic degeneration and mucinous cystic neoplasm (MCN) were the differential diagnoses.

Fluorodeoxyglucose-positron emission tomography (FDG-PET) revealed no FDG accumulation in the hepatic tumor and pancreatic cystic lesion, with no findings suggestive of

distant organ metastasis.

We performed an ultrasound-guided needle biopsy of the hepatic tumor, and the biopsy specimens showed solid and trabecular growth patterns that consisted of relatively uniform cells, finely granular eosinophilic cytoplasm, and a centrally located round to oval nucleus that may demonstrate a distinct nucleolus. This tissue was surrounded by a fibrous envelope that contained some degree of vessels and collagen fiber. Immunohistochemistry was positive for synaptophysin and CD56 with an MIB-1 labeling index of 14.0%. The definite diagnosis of PNEN with cystic change and liver metastasis was made.

Distal pancreatectomy, posterior segmentectomy, and five-part enucleation of the small liver metastasis, which had not been detected on preoperative imaging, were performed

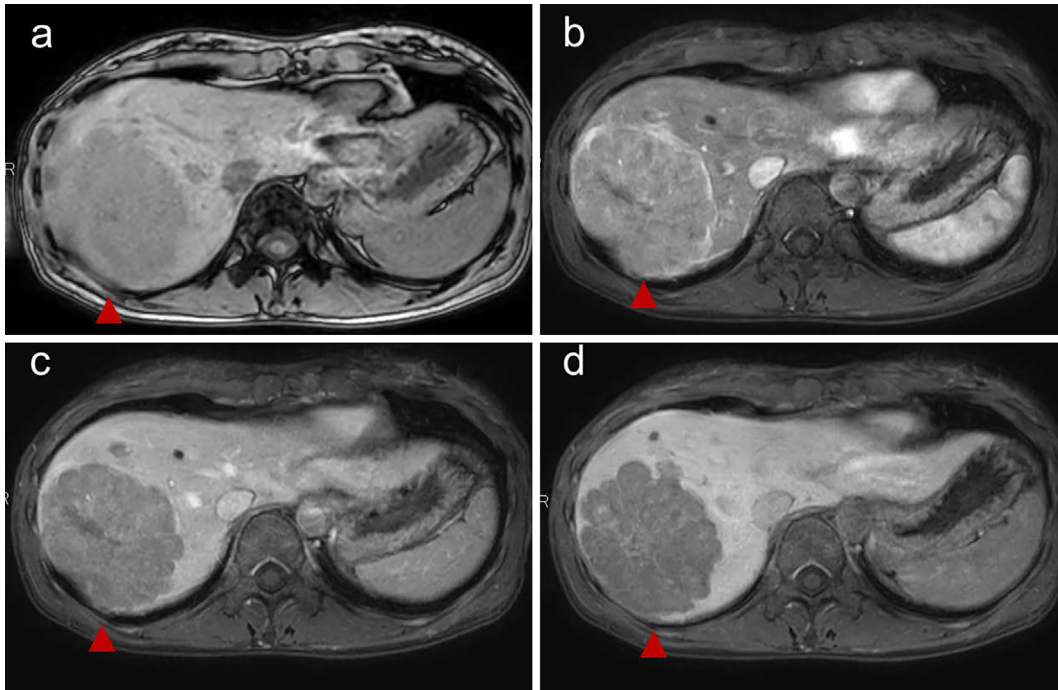


Figure 3. EOB-MRI: the hepatic tumor (triangle) demonstrated early enhancement with a poor-contrast central scar-like structure and washout during the portal venous and hepatobiliary phases. a: T1WI without contrast, b: arterial phase, c: portal venous phase, d: hepatobiliary phase. EOB-MRI: gadoxetic acid enhanced magnetic resonance imaging



Figure 4. EUS: A 24-mm sized cystic lesion with lateral shadowing and isoechoic and anechoic components is observed. Communication between the cyst and the main pancreatic duct is not seen. Contrast-enhanced EUS shows distinct enhancement in the outer border of the cystic wall and solid inside component. EUS: endoscopic ultrasonography

(Fig. 5, 6). The final diagnosis of PNEN G1 (MIB-1 labeling index: 1.8%) and multiple G2 liver metastasis (MIB-1 labeling index: 15.4%) was also made. No lymph node metastases were detected. The multiple small liver metastases had almost the same MIB-1 labeling index as the huge one. They were unable to detect MDCT, EOB-MRI, or FDG-PET preoperatively; we therefore performed somatostatin receptor

scintigraphy (SRS) (Octreoscan[®], FUJIFILM, Tokyo, Japan) to look for other occult metastases after the surgery. SRS and gadolinium-enhanced MRI detected an occult lumbar spine metastasis (Fig. 7). In this case, SRS was more useful than FDG-PET to detect bone metastasis.

The patient received chemotherapy with everolimus 10 mg daily and lanreotide 120 mg once every 28 days. A

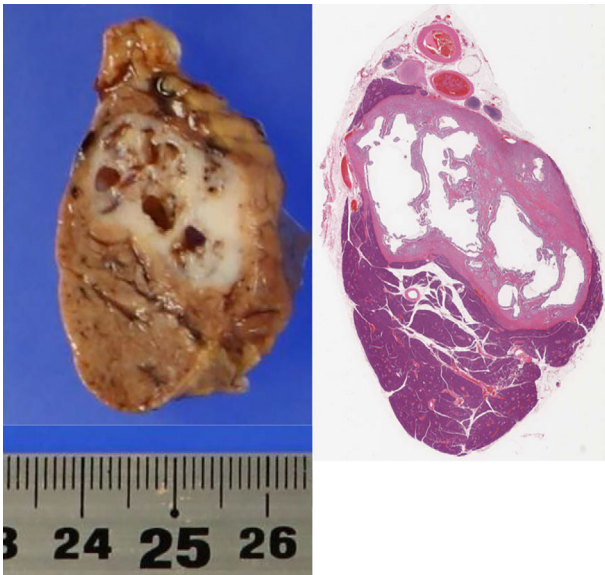


Figure 5. Distal pancreatectomy. The cystic neoplasm is growing not invasively but expansively to the adjacent pancreatic parenchyma. Small nests of endocrine tissue are present along the cystic wall. The superficial layers of endocrine cells are separated from the cystic lumen by a layer of fibrous tissue in continuity with the adjacent granulation tissue.

progression-free survival, as shown by trimonthly computed tomography (CT), was obtained for 10 months.

Discussion

PNENs usually have some typical features, such as solid, homogenous, and hypervascular. However, some cases like this have cystic components. Recent studies have investigated the demographics and clinicopathological characteristics of patients with cystic PNENs. These cystic subgroups account for approximately 5-36.1% of all resected PNENs (1-3). Despite the generally indolent nature, it has been recognized that the pathological potential is highly variable, and some cases present at an advanced stage with local invasion and distant metastases (4).

Several mechanisms have been suggested to explain cystic degeneration of PNENs. Historically, the presence of cystic change has been believed to be correlated with increasing tumor size. The increased size of the neoplasm may be due to the fact that the majority of lesions appear to be nonfunctional, so they grow until they are more symptomatic (5). Their development has been theorized to be related to cystic degeneration, secondary to either tumor necrosis or intralesional hemorrhaging (6). Bordeianou et al. reported that necrosis was encountered only occasionally, suggesting that necrosis may be a secondary phenomenon rather than the cause of cystic formation. They further noted that cystic PNENs are lined by a ragged cuff of well-preserved endo-

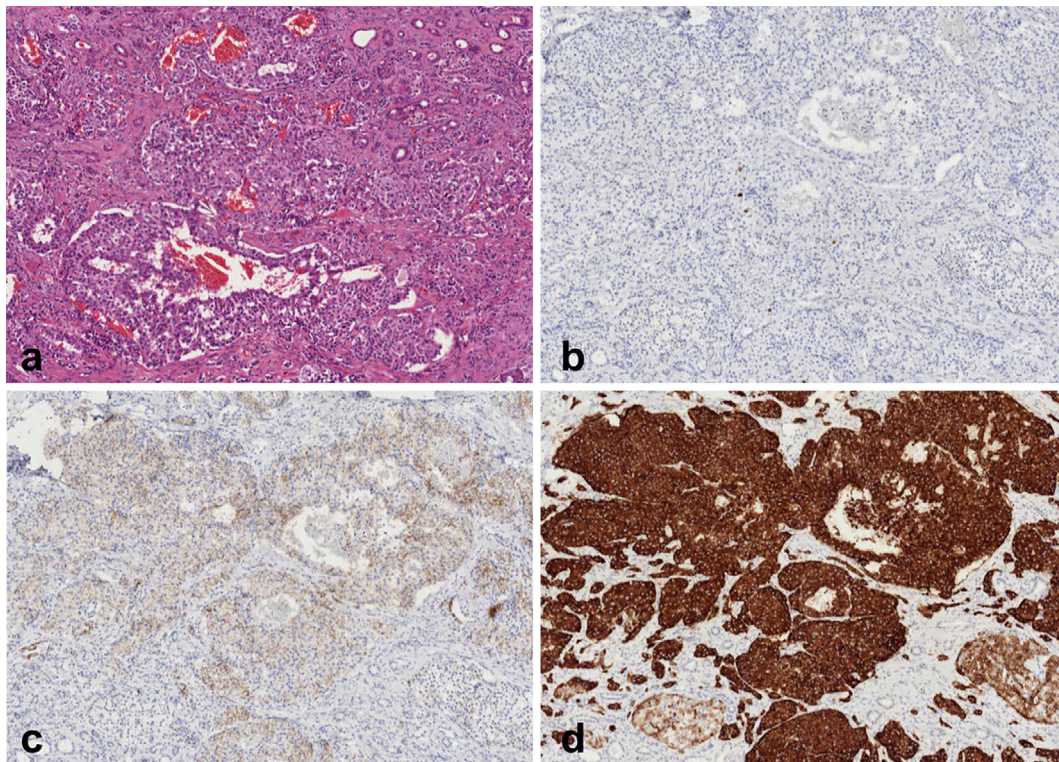


Figure 6. Pancreatic cystic neoplasm histopathology. Hematoxylin and Eosin staining: a solid and trabecular growth pattern consisting of relatively uniform cells, finely granular eosinophilic cytoplasm, and centrally located round-to-oval nuclei that may demonstrate a distinct nucleolus (a). Immunostaining was negative for chromogranin A (b) and positive for CD56 (c) and synaptophysin (d).

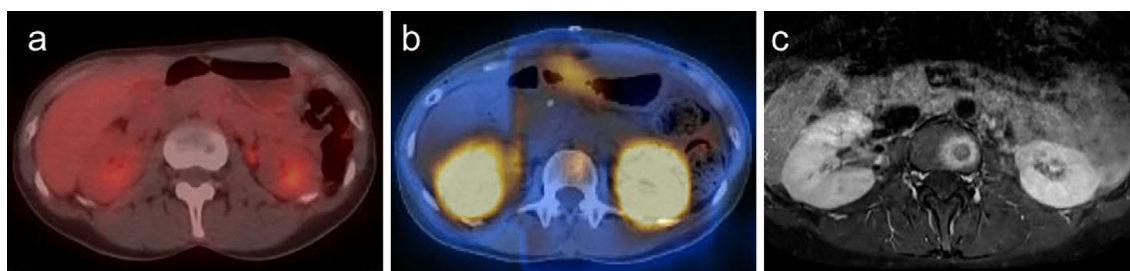


Figure 7. a: FDG-PET does not detect bone metastasis. b: SRS shows the abnormal accumulation in the second lumbar vertebra. c: Gadoteric acid-enhanced MRI confirms a nodule with a contrast effect. FDG-PET: fluorodeoxyglucose-positron emission tomography, SRS: somatostatin receptor scintigraphy

crine tumor, with the cavity filled with clear fluid instead of necrotic debris (3). Cystic PNENs were more likely to present as G1 and G2 rather than G3. They were associated with less frequent distant organ and lymph node metastasis, microvascular invasion, and perineural invasion as well as a low Ki-67 index and mitotic count and were less likely to be functional, more likely to affect men than women, and associated with MEN1 (2).

Given the gender, location, and gross appearance on CT and MRI, MCN was our primary diagnosis. MCN occasionally involves cysts appearing in part of the mother cyst. A nodule-like structure with a rounded cyst suggests malignancy. Our case showed an enhanced and thickened septal wall and nodule-like structure inside the cyst on EUS. These findings are characteristic of MCN, but distinct enhancement at the outer border of the cystic wall is suggestive of a solid component of cystic PNEN.

The present case is also interesting because of the presence of a huge liver metastasis for relatively small primary PNEN. We initially speculated that the hepatic tumor was a hepatic adenoma based on its contract pattern and her medical history of taking oral contraceptives. Furthermore, the morphology suggested FNH. These lesions are usually hyperenhanced in the early phase and isoenhanced in the hepatobiliary phase. However, a few cases of FNH have been reported to show defects during the delayed hepatobiliary phase (7).

We almost excluded hepatic cellular carcinoma due to the negative findings of tumor markers. We performed a needle biopsy from the hepatic tumor to distinguish hepatic adenoma, FNH, and pancreatic cyst neoplasm metastasis. The specimen confirmed the preoperative diagnosis of PNEN with cystic change and liver metastasis.

FDG-PET showed the accumulation of FDG in the liver metastasis but not in the other distant metastases. In contrast, SRS detected bone metastasis. We might have to consider performing SRS instead of FDG-PET preoperatively to search for occult metastasis. The SRS and FDG-PET sensitivity for NET-G2 is reported to be 96% and 73%, respectively (8). The usefulness of SRS, especially for extrahepatic metastases, has been reported. Frilling et al. reported that SRS was able to confirm liver metastases that had been de-

tected with other conventional imaging methods in all patients. In addition, 54.2% had extrahepatic tumor lesions not detected by other imaging techniques (9). SRS might be useful for identifying candidates suitable for resection.

Although SRS after surgery did not indicate residual liver metastasis, we suspected that there might be no somatostatin receptor. We performed histochemical staining of the somatostatin receptor for all resected liver tumors, and a high SSTR-2 expression was observed. These findings suggested that there were no residual tumors in the liver.

The present patient developed multiple systemic metastases; nevertheless, the primary tumor was G1. PNEN G1 is believed to be a less aggressive neoplasm than others. Lee et al. advocated for the nonoperative management of patients with incidental, small, nonfunctional PNENs up to 3 cm in size with Ki-67 values <5% based on a retrospective review of 77 patients who showed no evidence of significant tumor growth or disease progression at a mean follow-up of 45 months (10). Among patients with low-grade, small tumors measuring ≤ 2 cm, 1 of 39 patients (2.6%) had disease recurrence and eventually died (11). Zou et al. reported on the prognosis after curative surgery; recurrence was observed in 2.9% (5/173) of patients in PNEN G1 (12). Sadot et al. stated that, in 77 patients with PNENs ≤ 3 cm in size, including 72 patients with G1, 1 had lymph node-positive disease, and 5 developed recurrence after surgery (13). Our present patient had multiple G2 liver metastases as well as a G1 pancreatic neoplasm. The mitotic count varied in the pancreatic neoplasm, and vascular invasion was seen. A highly mitotic tumor component in the pancreas may have metastasized to the liver and bone. Discordance between the liver metastasis and primary site has been reported. In addition, 24% of cases reportedly showed the elevation of the Ki-67 labeling index in metastases. When the grade increased, both the progression-free survival and overall survival significantly decreased (14).

Conclusion

Cystic degeneration of PNEN requires a differential diagnoses. In addition, although the cystic PNEN in the present study was G1 and seemed to be indolent, the liver tumor was G2, with multiple lesions, enhancement in an uncom-

mon pattern, and a huge size relative to the primary pancreatic neoplasm. Bone metastasis was also detected. In the present case, SRS was more useful than FDG-PET for detecting bone metastasis. We encountered a rare case of G1 cystic PNEN with liver and bone metastases of the G2 component.

The authors state that they have no Conflict of Interest (COI).

References

1. Edwin B, Mala T, Mathisen Ø, et al. Laparoscopic resection of the pancreas: a feasibility study of the short-term outcome. *Surg Endosc* **18**: 407-411, 2004.
2. Zhu JK, Wu D, Xu JW, et al. Cystic pancreatic neuroendocrine tumors: a distinctive subgroup with indolent biological behavior? A systematic review and meta-analysis. *Pancreatol* **19**: 738-750, 2019.
3. Bordeianou L, Vagefi PA, Sahani D, et al. Cystic pancreatic endocrine neoplasms: a distinct tumor type? *J Am Coll Surg* **206**: 1154-1158, 2008.
4. Bilimoria KY, Talamonti MS, Tomlinson JS, et al. Prognostic score predicting survival after resection of pancreatic neuroendocrine tumors: analysis of 3851 patients. *Ann Surg* **247**: 490-500, 2008.
5. Buetow PC, Parrino TV, Buck JL, et al. Islet cell tumors of the pancreas: pathologic-imaging correlation among size, necrosis and cysts, calcification, malignant behavior, and functional status. *AJR Am J Roentgenol* **165**: 1175-1179, 1995.
6. Koh YX, Chok AY, Zheng HL, Tan CS, Goh BK. A systematic review and meta-analysis of the clinicopathologic characteristics of cystic versus solid pancreatic neuroendocrine neoplasms. *Surgery* **156**: 83-96.e2, 2014.
7. Yoon JH, Kim JY. Atypical findings of focal nodular hyperplasia with gadoxetic acid (Gd-EOB-DTPA)-enhanced magnetic resonance imaging. *Iran J Radiol* **11**: e9269, 2014.
8. Binderup T, Knigge U, Loft A, et al. Functional imaging of neuroendocrine tumors: a head-to-head comparison of somatostatin receptor scintigraphy, 123I-MIBG scintigraphy, and ¹⁸F-FDG PET. *J Nucl Med* **51**: 704-712, 2010.
9. Frilling A, Malago M, Martin H, Broelsch CE. Use of somatostatin receptor scintigraphy to image extrahepatic metastases of neuroendocrine tumors. *Surgery* **124**: 1000-1004, 1998.
10. Lee LC, Grant CS, Salomao DR, et al. Small, nonfunctioning, asymptomatic pancreatic neuroendocrine tumors (PNETs): role for nonoperative management. *Surgery* **152**: 965-974, 2012.
11. Haynes AB, Deshpande V, Ingkakul T, et al. Implications of incidentally discovered, nonfunctioning pancreatic endocrine tumors: short-term and long-term patient outcomes. *Arch Surg* **146**: 534-538, 2011.
12. Zou S, Jiang Y, Wang W, Zhan Q, Deng X, Shen B. Novel scoring system for recurrence risk classification of surgically resected G1/2 pancreatic neuroendocrine tumors - Retrospective cohort study. *Int J Surg* **74**: 86-91, 2020.
13. Sadot E, Reidy-Lagunes DL, Tang LH, et al. Observation versus Resection for Small Asymptomatic Pancreatic Neuroendocrine Tumors: A Matched Case-Control Study. *Ann Surg Oncol* **23**: 1361-1370, 2016.
14. Keck KJ, Choi A, Maxwell JE, et al. Increased grade in neuroendocrine tumor metastases negatively impacts survival. *Ann Surg Oncol* **24**: 2206-2212, 2017.

The Internal Medicine is an Open Access journal distributed under the Creative Commons Attribution-NonCommercial-NoDerivatives 4.0 International License. To view the details of this license, please visit (<https://creativecommons.org/licenses/by-nc-nd/4.0/>).